

Thermal analysis of phase change emulsion

T. Kousksou · A. Jamil · S. Gibout ·
Y. Zeraouli

Received: 10 January 2008 / Accepted: 20 March 2009 / Published online: 3 July 2009
© Akadémiai Kiadó, Budapest, Hungary 2009

Abstract This paper presents some results obtained by Differential Scanning Calorimetry (DSC) for characterizing the phase transition within an emulsion. The dispersed substances are either hexadecane, octadecane, water or binary solution. A non-equilibrium model taking into account the inter-phase heat transfer between the emulsifying medium and the dispersed droplet is proposed and explains the main experimental features.

Keywords Binary solution · DSC · Emulsion · Paraffin · Phase change micro-cell

Nomenclature

c	Specific heat capacity ($\text{J kg}^{-1}\text{K}^{-1}$)
f	Liquid fraction
h	Exchange coefficient for the droplet ($\text{W m}^{-2}\text{K}^{-1}$)
h_1, h_2	External exchange coefficient for the cell ($\text{W m}^{-2}\text{K}^{-1}$)
k	Thermal conductivity ($\text{W m}^{-1}\text{K}^{-1}$)
L_D	Heat of dissolution of salt in the solution (J kg^{-1})
L_F	Melting heat (J kg^{-1})
P	Mass fraction of the dispersed solution
X	Transformed fraction

X_E	Eutectic concentration
X_{ic}	Ice mass fraction
X_s	Solid fraction
T	Temperature (K)

Greek symbols

β	Heating rate ($^{\circ}\text{C min}^{-1}$)
ΔS	Surface (m^2)
ρ	Density (kg m^{-3})
ε	Porosity
Φ	Heat flow rate (W kg^{-1})

Subscripts

a	Antifreeze
E	Eutectic
em	Emulsion
f	Emulsifying medium
i	Initial
ic	Ice
m	Melting
pcm	Phase change material
plt	Plate
s	Solid

Introduction

Emulsions, which are systems made of liquid droplets dispersed in another one with which it is incompletely miscible, have been subject of intensive study for many years as a result of very interesting properties they display [1–6].

Our research team (see Refs. [7–12]) has already presented numerical and experimental results concerning the heat transfer during the crystallization and the melting of the droplets dispersed within an emulsion. The two processes are not symmetrical because of the supercooling

T. Kousksou (✉) · S. Gibout · Y. Zeraouli
Laboratoire de Thermique Energétique et Procédés,
Avenue de l'Université, BP 1155, 64013 Pau Cedex, France
e-mail: Tarik.kousksou@univ-pau.fr

A. Jamil
Cemagref, Groupement d'Antony, Parc de Tourvoie,
BP 44, 92163 Antony Cedex, France

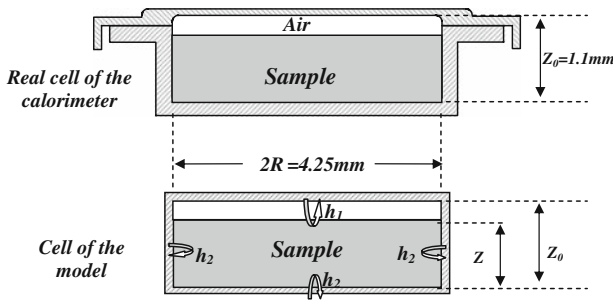


Fig. 1 Experimental cell and scheme for the model

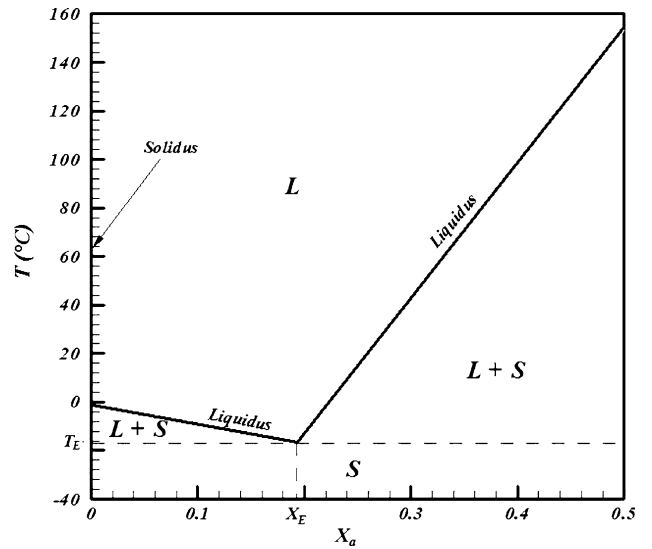


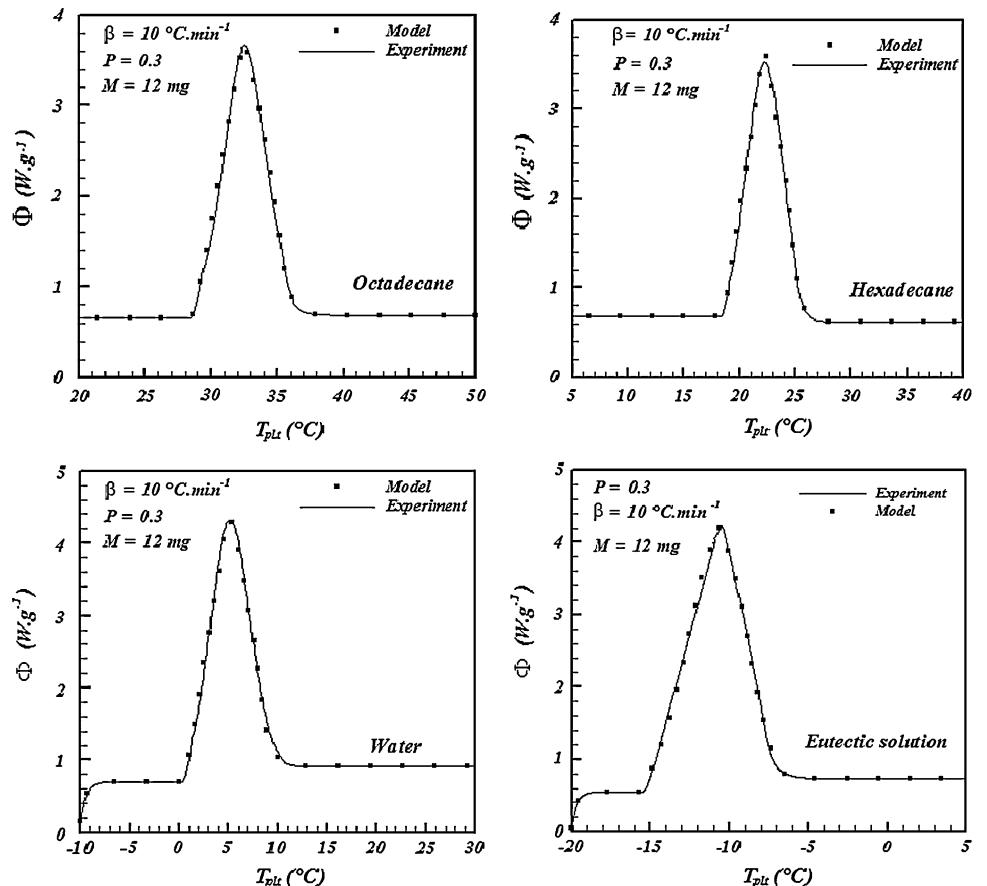
Fig. 2 Phase diagram for a binary solution (NH₄Cl–H₂O)

phenomenon induced by the smallness of the emulsion droplets sizes. At the crystallization the release of energy, for a droplet, is practically instantaneous because it occurs far from the thermodynamic equilibrium but at the melting, the absorption of energy is at the fixed melting temperature and its kinetics depends on the exchanges with the surrounding medium.

In this paper we present a review of some results obtained by Differential Scanning Calorimetry (DSC) for characterizing the melting of the dispersed droplets in the emulsions. The effect of different parameters such as the

phase change material, the heating rate, the mass fraction, the sample mass is analysed. A comparison will be made with experimental results.

Fig. 3 Theoretical and experimental curve ($P = 0.3$, $M = 12 \text{ mg}$ $\beta = 10 \text{ }^\circ\text{C}\cdot\text{min}^{-1}$)



Experimental

Investigated materials

The investigated substances are Analytic Grade paraffins such as hexadecane ($T_m = 18.0\text{ }^\circ\text{C}$) or octadecane ($T_m = 27.5\text{ }^\circ\text{C}$), distilled water and $\text{NH}_4\text{CL-H}_2\text{O}$ binary eutectic system. They are dispersed by a high speed stirrer within an emulsifying medium made of a mixture of water, glycerol and Tween 80^R as surfactant for the paraffins and a mixture of paraffin oil and lanolin for water and $\text{NH}_4\text{CL-H}_2\text{O}$ binary eutectic system. For hexadecane, by a particular choice of the relative concentrations of the constitutive substances of the emulsifying medium, the dispersed system is, in fact, a microemulsion. So, it is very stable. Emulsions were elaborated in a special tank to prevent any segregation and to obtain a homogeneous mixture. To maintain a constant temperature during experiments, and to be able to control it, the stirring tank

was placed into a thermostated vessel. It was necessary that the emulsion retain its characteristics when it came into contact with the walls of the crucible for the calorimeter.

DSC is one of the most widely used analytical instruments because of the ease with which it can provide large amounts of thermodynamic data. From a single DSC test that consists in regularly cooling down and heating of a sample, it is expected to obtain qualitative and quantitative information on the phase transitions of a sample, such as transition temperature, enthalpy, heat capacity, specific heat, and latent heat.

In this work, thermal analysis was carried out using a PYRIS DIAMOND DSC of Perkin-Elmer. The temperature scale of the instrument was calibrated by the melting point of pure ice (273.15 K or $0\text{ }^\circ\text{C}$) and mercury (234.32 K or $-38.82\text{ }^\circ\text{C}$). The principle of the power-compensation used in dispersed droplet is widely detailed in Refs. [11, 12].

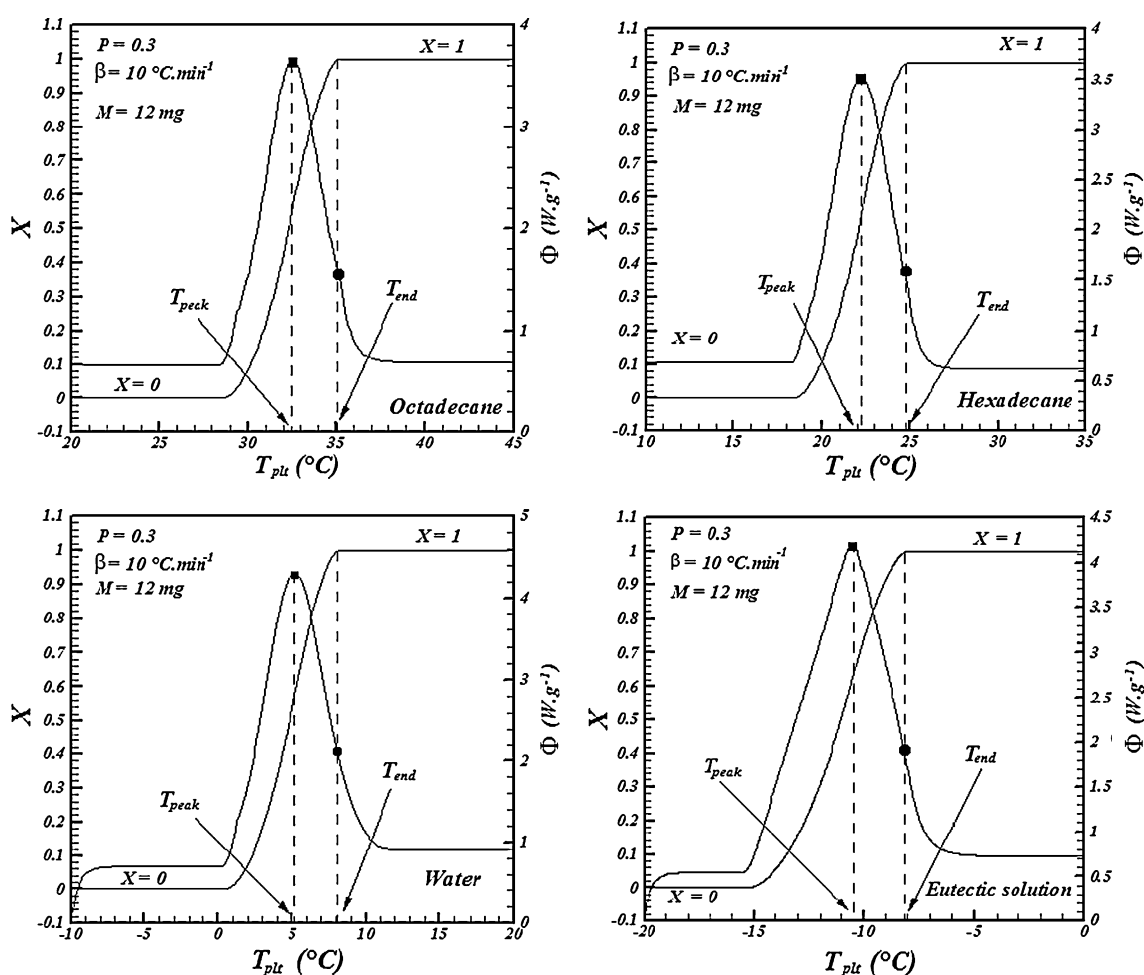


Fig. 4 Transformed fraction vs. T_{plt}

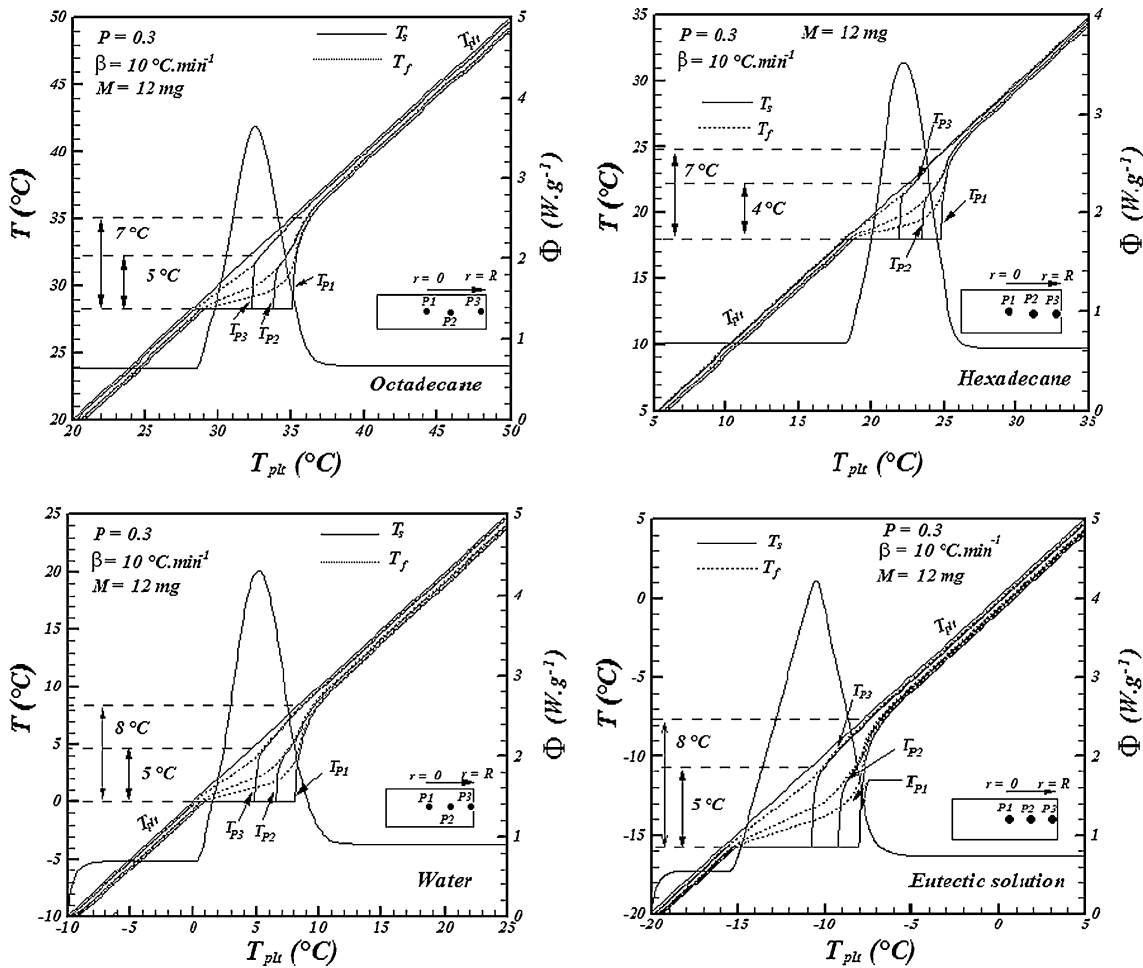


Fig. 5 T_f and T_{pcm} vs. radius r ($P = 0.3$, $M = 12 \text{ mg}$, $\beta = 10 \text{ }^\circ\text{C}\cdot\text{min}^{-1}$)

In Fig. 1, we have drawn the real cell and the simplified scheme used in our model. The sample fills a cylindrical cell of height $Z_0 = 1.1 \text{ mm}$ and radius $R = 2.125 \text{ mm}$.

Equilibrium phase diagram of the $\text{NH}_4\text{Cl}-\text{H}_2\text{O}$ system

Figure 2 shows the equilibrium phase diagram for the $\text{NH}_4\text{Cl}-\text{H}_2\text{O}$ system, which has a eutectic temperature and concentration of $T_E = -15.7 \text{ }^\circ\text{C}$ and $X_E = 0.195$ respectively. The symbols L , S and $L + S$ denote the liquid phase, the solid phase and the solid-liquid two phase, respectively.

In our application the over-eutectic part is not of interest. If the solute mass fraction X_a is lower than X_E the ice mass fraction X_{ic} can be calculated from the liquidus temperature of the binary mixture solution, which is function of X_a .

$$T = T(X_a) \tag{1}$$

Once the initial mass fraction of the solute in the binary mixture solution before freezing $X_{a,i}$ and temperature are known, the equilibrium ice mass fraction is calculated with:

$$X_{ic} = 1 - \frac{X_{a,i}}{X_a(T)} \tag{2}$$

In which $X_a(T)$ is found from the liquidus curve, the inverse of Eq. 1.

Theoretical model

The droplets of emulsion are so small ($1 \text{ }\mu\text{m}^3$ in volume), the dispersed system is so viscous and the variation of density is so small, that the possible convective diffusion inside the droplets during the phase transition, does not involve a movement of emulsion as a whole. So, only the conduction must be taken into account.

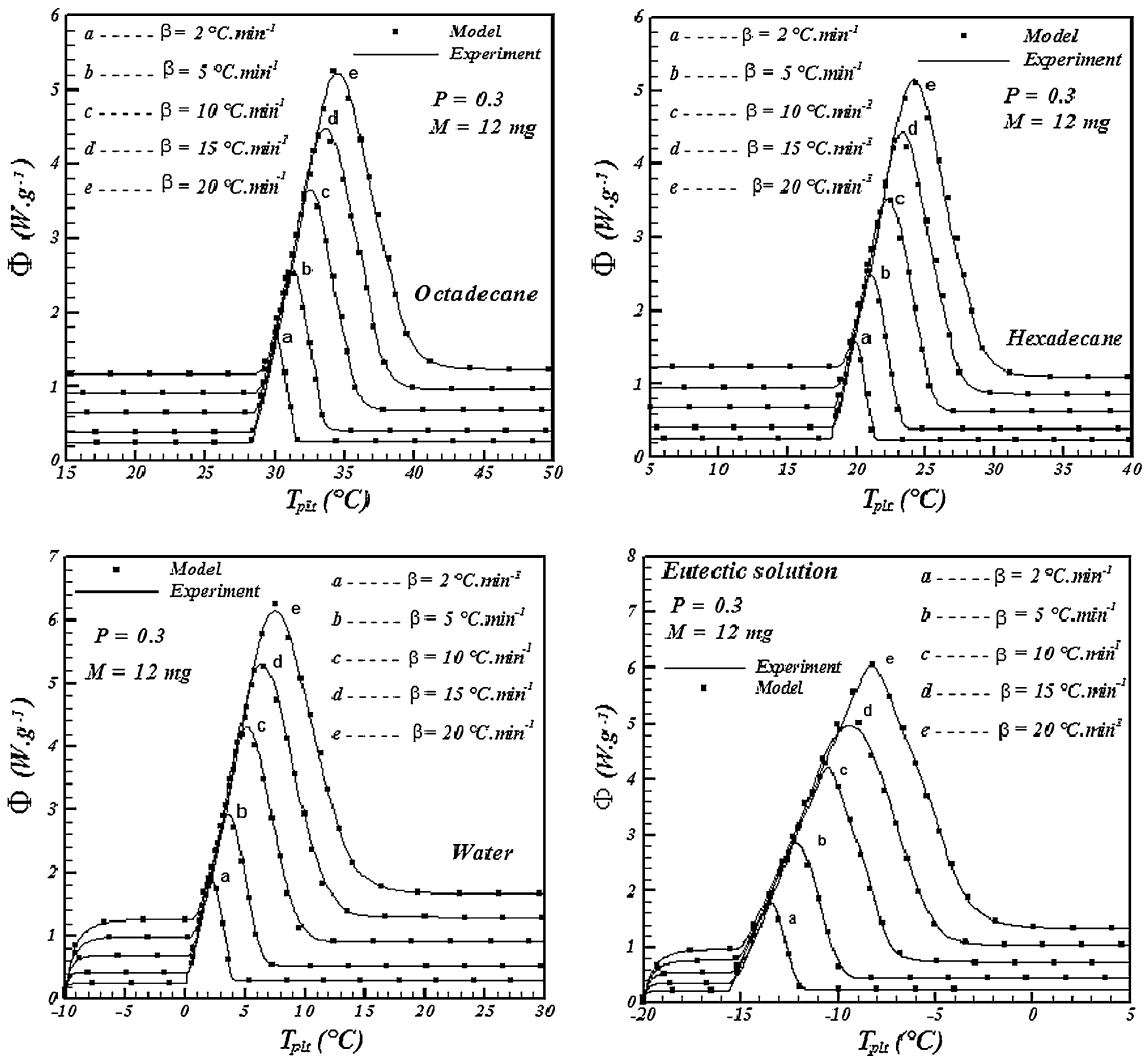


Fig. 6 Effect of the heating rate on the shape of curve ($P = 0.3, M = 12 \text{ mg } \beta = 10 \text{ }^\circ\text{C}\cdot\text{min}^{-1}$)

To study the melting process inside an emulsion, we assume that the emulsifying medium and the droplet are not in local thermodynamic equilibrium and therefore, a two temperature model of microscopic heat transfer applies. The governing equations for the emulsifying medium and the solution temperatures are:

$$\varepsilon(\rho c)_f \frac{\partial T_f}{\partial t} = \varepsilon k_f \nabla^2 T_f + h(T_{pcm} - T_f) \tag{3}$$

$$(1 - \varepsilon)(\rho c)_{pcm} \frac{\partial T_{pcm}}{\partial t} = h(T_f - T_{pcm}) \tag{4}$$

Where T is the temperature, ρ the mass density, c the specific heat, k the thermal conductivity, h is the overall constant heat transfer coefficient, f and pcm subscripts denote the emulsifying medium and PCM phases respectively and ε is the porosity defined by the following relation:

$$\varepsilon = 1 - P \frac{\rho_{em}}{\rho_{pcm}} \tag{5}$$

Where P is the mass fraction of the emulsion defined as the ratio between the mass of the dispersed solution and the mass of the emulsion. ρ_{em} is the mass density of the emulsion.

During the isothermal melting (i.e. eutectic melting), the energy balance is quite different because $T_{pcm} = T_m$ and the exchanged heat proceeds from the fraction of crystal which is melting:

$$(1 - \varepsilon)\rho_{pcm}A \frac{\partial X_s}{\partial t} = -h(T_f - T_E) \tag{6}$$

X_s indicates the solid mass fraction. The coefficient A is given by:

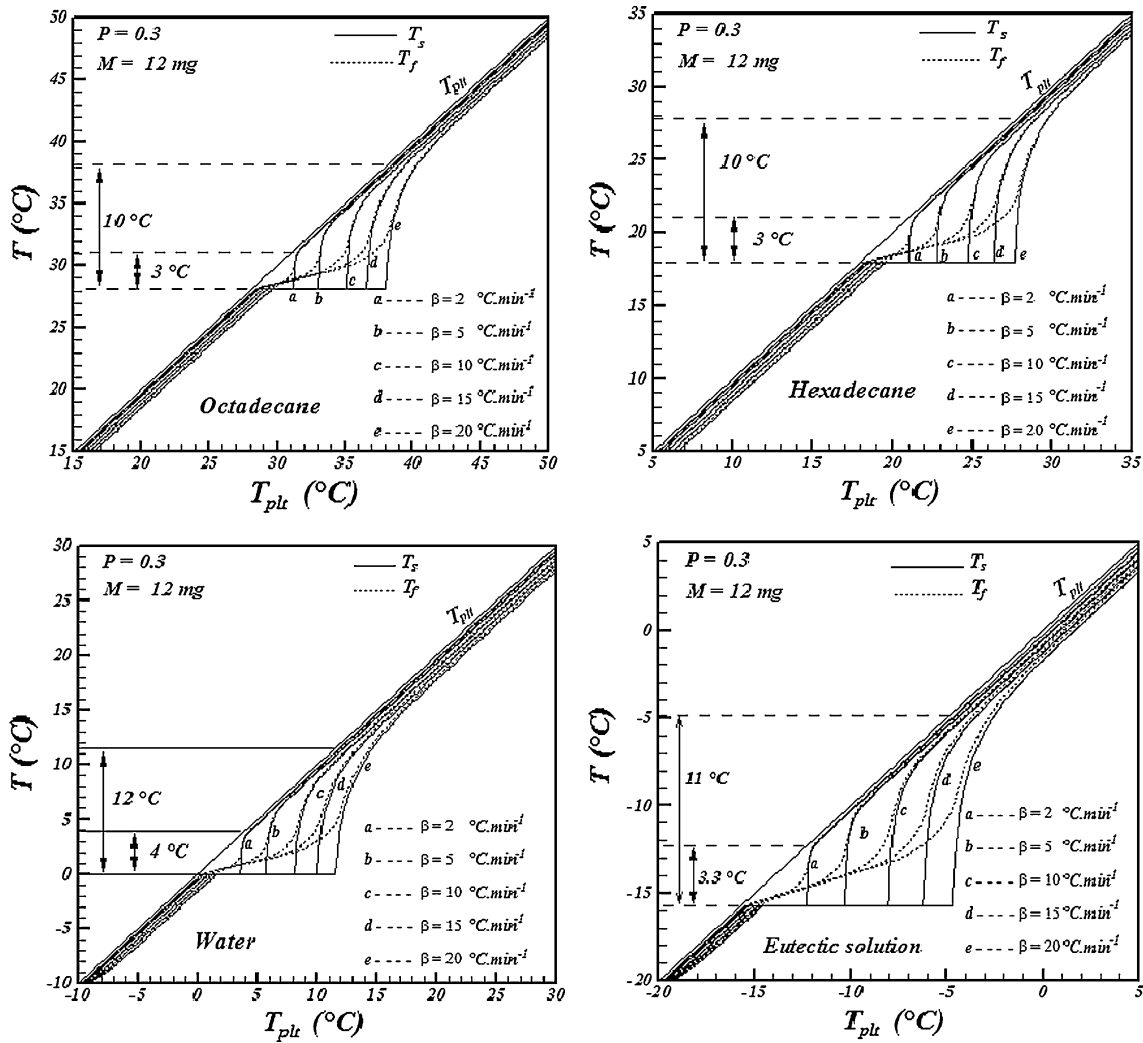


Fig. 7 Influence of the heating rate β on T_f , T_{pcm} and X_g in the center of the sample

$A = L_F(T)$ when the cell is filled by the pure sample (hexadecane, octadecane or water)

$$A = L_F(T) + \frac{X_E}{1 - X_E} L_D \text{ for the binary solution (NH}_4\text{Cl-H}_2\text{O)}$$

Where L_F and L_D represent the latent heat of fusion and the dissolution heat in the formed solution respectively.

During the non-isothermal melting (i.e. progressive melting), the appropriate equation for the eutectic mixture (NH₄Cl-H₂O) is

$$(1 - \varepsilon)\rho_{pcm}c_{pcm} \frac{\partial T_{pcm}}{\partial T} = (1 - \varepsilon)\rho_{pcm}L_F \frac{\partial X_S}{\partial t} + h(T_f - T_{pcm}) \tag{7}$$

In the above equation the unknowns are only the temperatures T_{pcm} because the solid mass fractions X_s are themselves function of the temperatures according the Eq. 2.

To take into account the air between the sample and the cover of the cell, we consider two different heat exchange coefficient h_1 and h_2 . So, the boundaries conditions are:

$$\left(\frac{\partial T}{\partial r}\right)_{r=0} = 0 \tag{8}$$

$$-k_f \left(\frac{\partial T}{\partial r}\right)_{r=R} = h_2(T - T_{plt}) \tag{9}$$

$$-k_f \left(\frac{\partial T}{\partial r}\right)_{z=0} = h_2(T - T_{plt}) \tag{10}$$

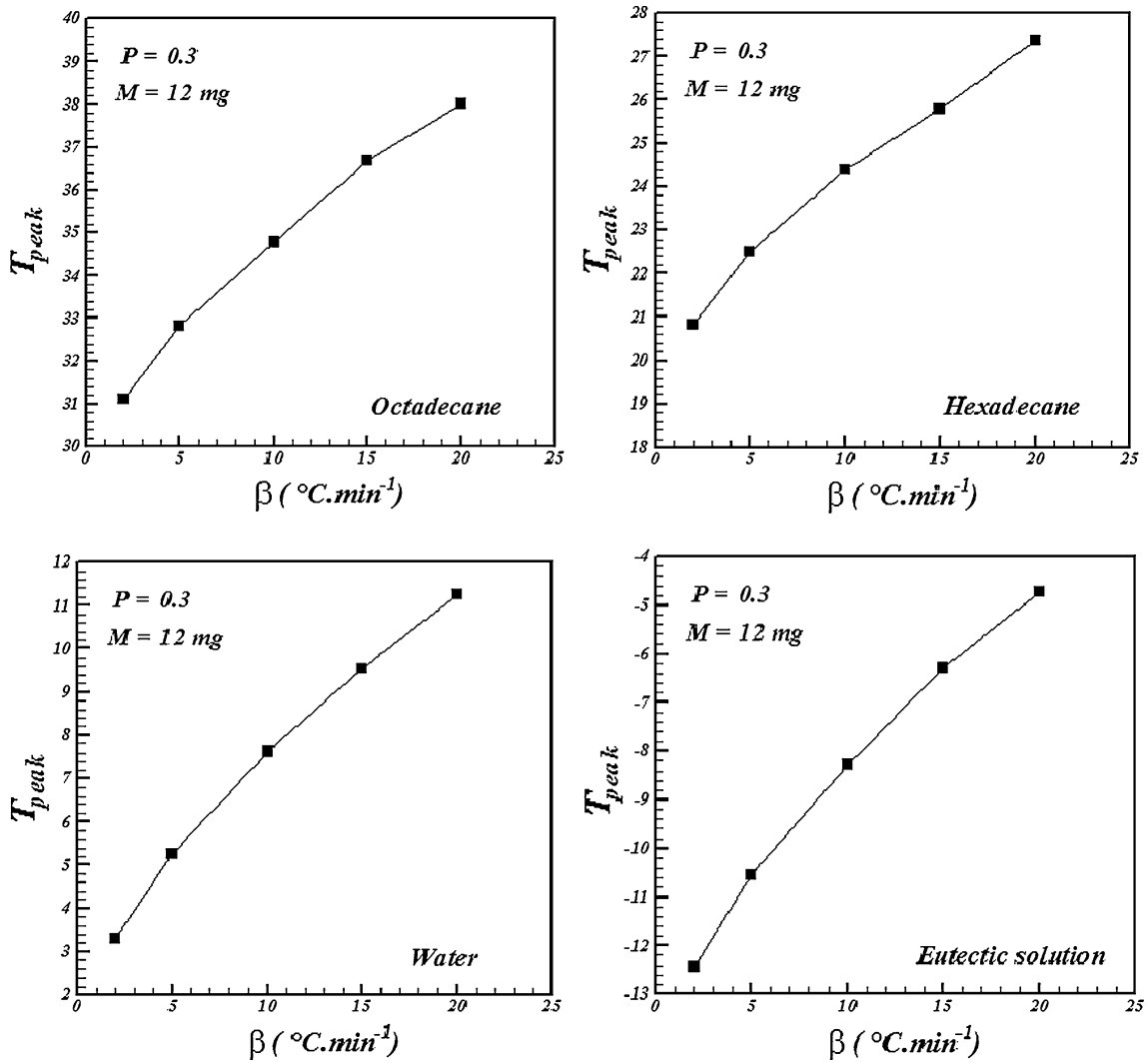


Fig. 8 T_{peak} for different heating rate

$$-k_f \left(\frac{\partial T}{\partial r} \right)_{z=Z} = h_2(T - T_{plt}) \tag{11}$$

Where T_{plt} , the temperature of the plates is programmed to be linear function:

$$T_{plt} = \beta t + T_0 \tag{12}$$

At $t = 0$ the initial conditions are $T(r,z,0) = T_0$ and $X_s(r,z,0) = 0$

Because the thermal conductivity of air is smaller than that of the metal of the cell, we consider that all the energy is transmitted to the plate by the lower boundary of the cell. So, Φ is the sum of the thermal fluxes through the walls of the metallic cell.

$$\Phi = - \sum_i h_i(T_i - T_{plt})\Delta S_i \tag{13}$$

Where $h_i = h_1$ or h_2

By use of this model, it is possible to study the effect of various parameters on the melting kinetic inside an emulsion.

Results and discussion

Thermal analyses were carried out using a Pyris Diamond DSC of Perkin-Elmer. The temperature scale of the instrument was calibrated by the melting point of pure ice (273.15 K) and mercure (234.32 K). The DSC experiments were conducted by placing the emulsion in the aluminium DSC cell. The sample was cooled at $2^{\circ}\text{C}\cdot\text{min}^{-1}$ until

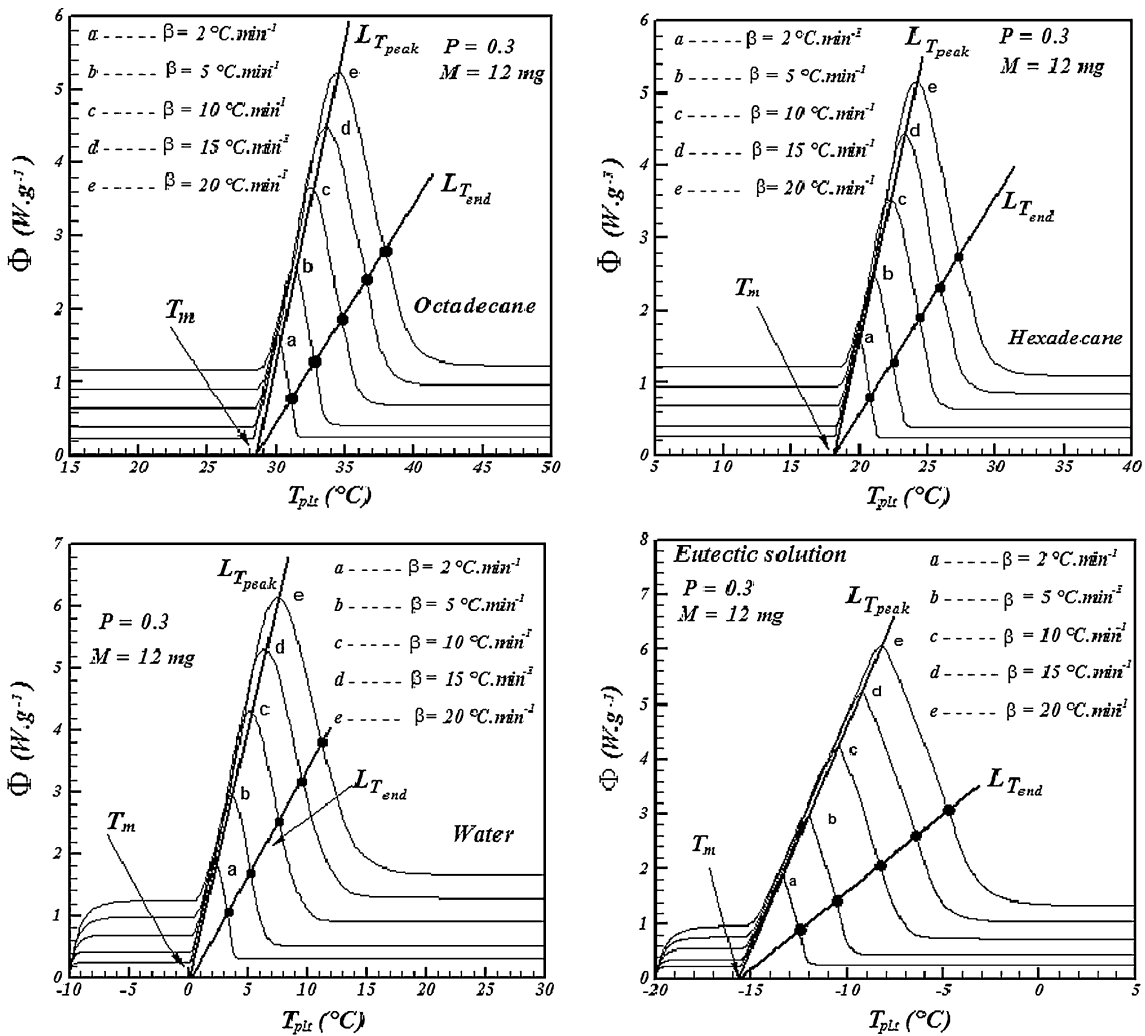


Fig. 9 Determination of melting temperature

crystallization of the dispersed droplets. The sample was then heated at various heating rate.

For the numerical calculation, we have applied the theoretical model described in the previous section. The values of the physical characteristics required in different equations have been determined experimentally or using the literature correlations [13], except the coefficients of heat exchange (h_1, h_2 and h) that have been determined by simulation from exploratory experiments.

In the present work, we present only the numerical and experiment results for water, octadecane, hexadecane and the eutectic solution $\text{NH}_4\text{Cl}-\text{H}_2\text{O}$ at $X_{a,i} = 0.1965$.

A comparison of the experimental and numerical curves is given in Fig. 3. Good agreement can be seen in the results. Naturally, no two phase region emerges for ($X_{a,i} = 0.1965, T_E = 15.7$ °C) and the shape of the curve is similar to that for ordinary pure PCM.

The advantage of the model is that it permits the calculation at each instant the liquid fraction of the PCM inside the emulsion. During the melting process, the liquid fraction of PCM inside the sample reaches 1 for (hexadecane, octadecane, water and the eutectic solution) and this taken as the end point of phase transformation Fig. 4.

Figure 5 presents the temperatures T_f and T_{pcm} inside the emulsion at different points of the cell versus T_{plt} . Important temperature differences can be observed as a function of the radius or the height of the cell. There is a small difference between the temperature of the emulsifying medium and the PCM temperature.

Effect of the heating rate β

Figure 6 shows the curves obtained by the model and DSC for various heating rate. The melting temperatures range

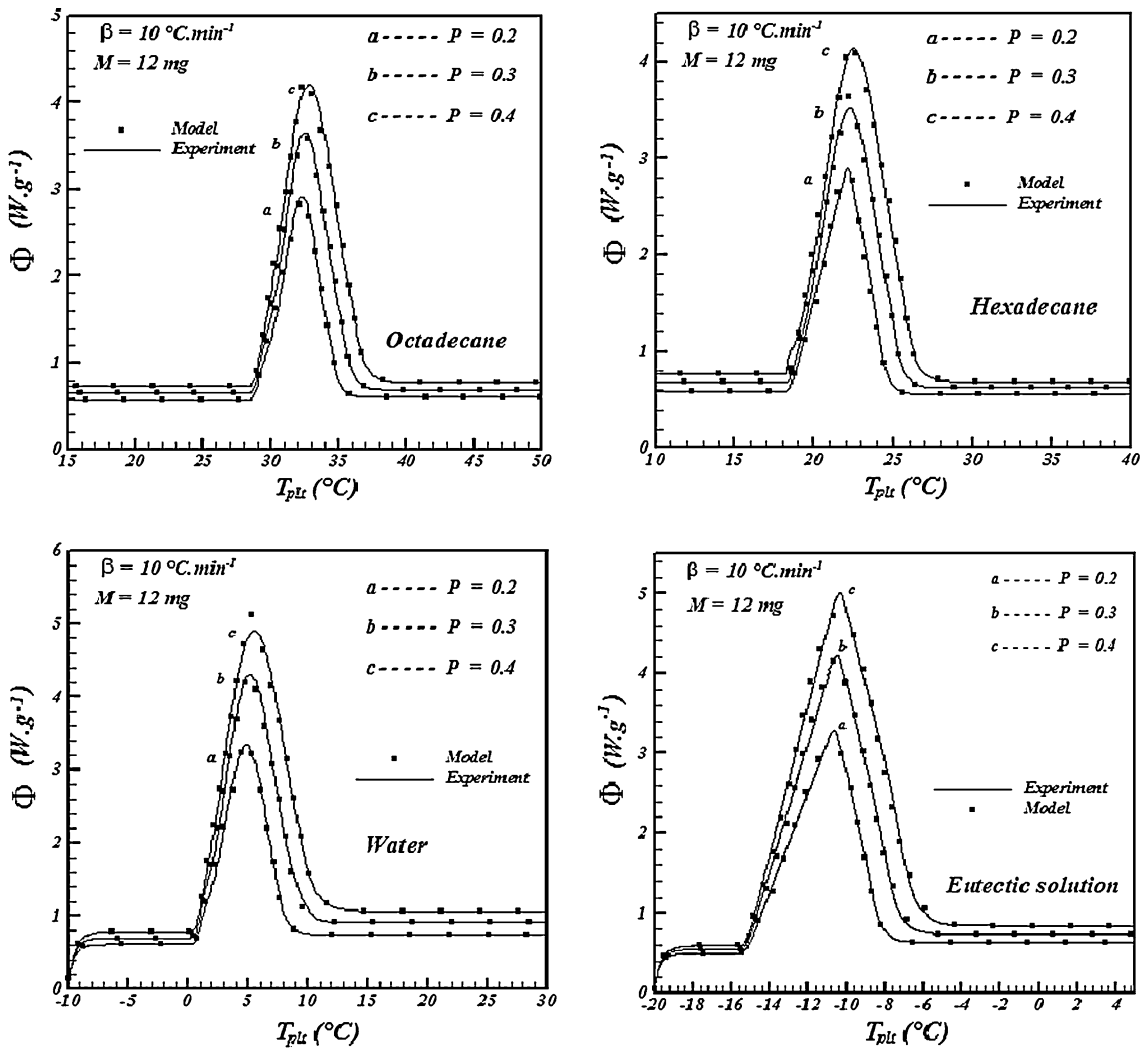


Fig. 10 Influence of the mass fraction P on the shape of curves

becomes broader and it shifts to greater temperature with increasing heating rate. We can also note that the peak maximum temperature T_{peak} increase continuously which increasing heat rate.

Figure 7 displays the prediction of temperatures T_f and T_{pcm} versus T_{plt} in the center of the sample for different heating rate. It can be seen from this figure that the temperature differences inside the sample becomes more important as the heating rate increases.

Figure 8 gives the calculated values of T_{end} for different values of the heating rate β . We observe that T_{end} decreases when β increases but T_{end} is not a linear function of β . This effect on the end temperatures is caused by the overall thermal resistance (both between the cell and the DSC plate from and within the sample).

From Fig. 9, it is found that for different heating rates all points, whose abscissa is, T_{end} form a line $L_{T_{end}}$, which cuts the axis of abscissas to $T_{plt} = T_m$. This temperature corresponds exactly to the melting temperature for water, octadecane, hexadecane and to the eutectic temperature for the eutectic solution NH_4Cl-H_2O . The same result is obtained for T_{peak} . We find that for various heating rates all points whose abscissa is T_{peak} are aligned. The straight line $L_{T_{peak}}$ formed by these points cuts also the axis of abscissas to $T_{plt} = T_m$. We note also that the intersection of the two lines ($L_{T_{end}}$ and $L_{T_{peak}}$) given on the axis of abscissa coincides with the melting temperature of the PCM and indicates the limit of the curve when $\beta \rightarrow 0$.

These results can be explained by the fact that more the heating rate decreases and become near to zero, the more

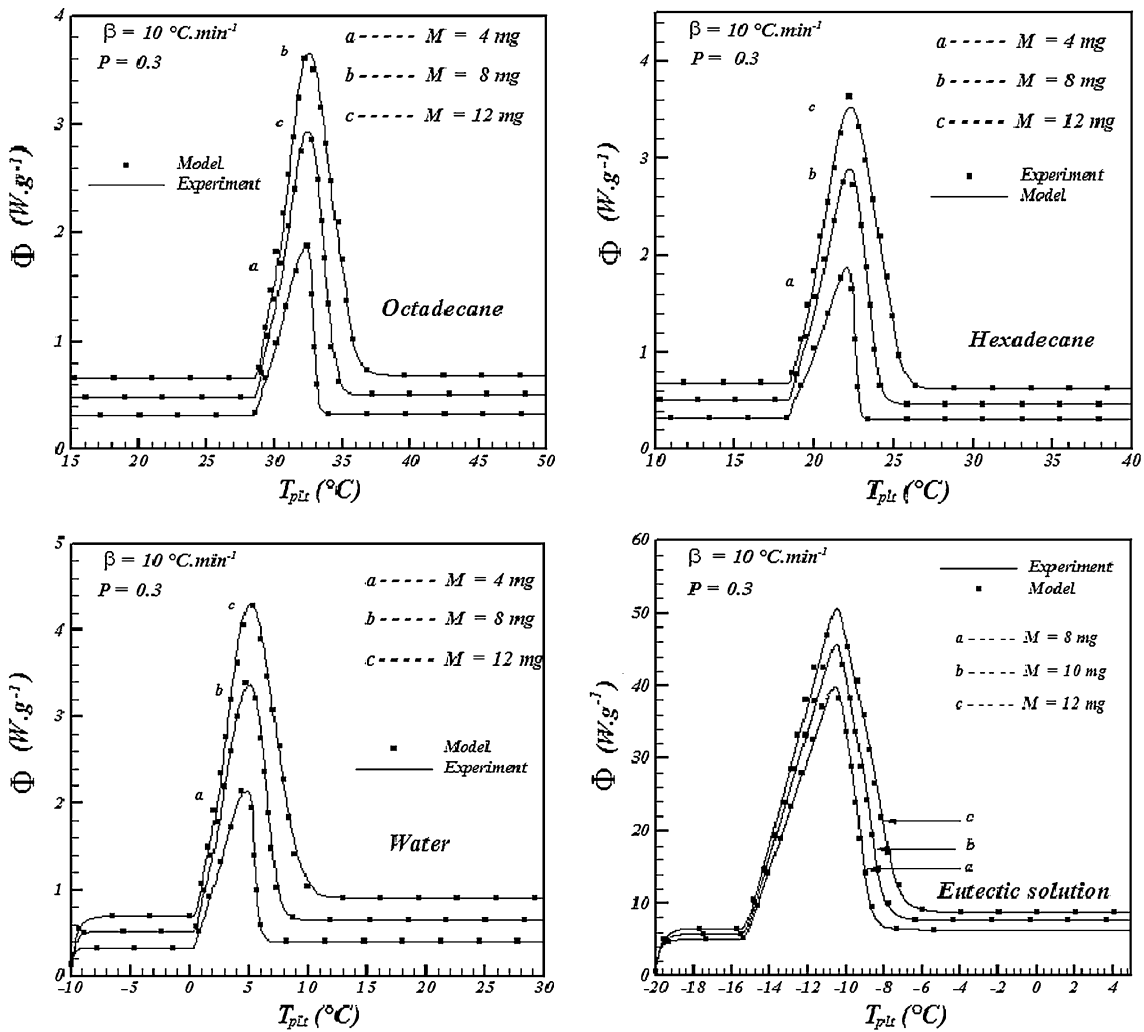


Fig. 11 Influence of the mass on the shape of curves

the gradients of temperature within the sample become negligible. In the case of the smaller heating rates the end point of the phase transformation corresponds practically to the maximum peak. In this case, the melting temperature can be taken as the peak temperature. The discrepancy between the peak temperature and the end temperature become significant when the heating rate increases. For the high heating rates, the melting temperature of the PCM can be determined from the intersection of the two lines ($L_{T_{end}}$ and $L_{T_{peak}}$).

Effect of the mass fraction P

We have plotted curves giving by the experimental and theoretical curves versus the mass fraction P (see Fig. 10). As can be seen the kinetics of the melting process depends

on P . We notice that the rise in the mass fraction P leads to an increase in the mass of the dispersed PCM inside the emulsion. As the rise in the percentage of PCM increases the time required for the melting process, the peak temperatures range becomes broader and its shifts to greater temperatures with increasing the mass fraction P .

Effect of the sample mass

From the numerical and experimental analysis, we can present the non-normalized heat flow for different mass of the sample at a fixed heating rate, as one can see in Fig. 11. In these plots we found that the peak temperature increases with increasing the mass sample. The temperature inside the sample becomes more important as the sample mass increases (see Fig. 12).

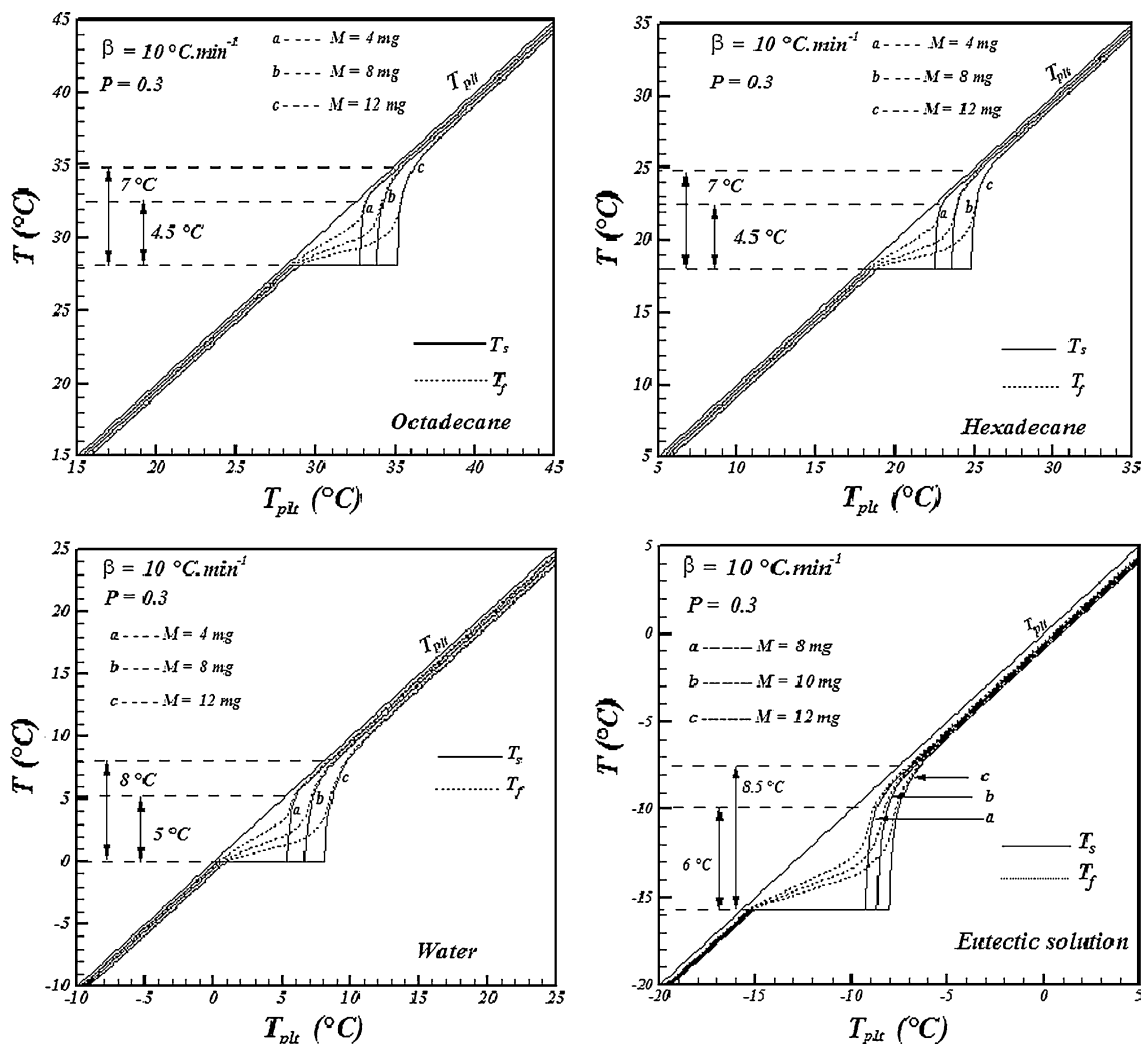


Fig. 12 Effect of the sample mass on the T_f and T_{pcm} in the center of the sample

Conclusions

In this article, heat transfer inside a phase change emulsion in the heating mode for different dispersed substances, such as hexadecane, octadecane, water and binary solution is studied. We have also investigated the effect of various parameters: sample masses, mass fraction and various heating rates on the melting process. Finally, recommendations are proposed concerning the determination of the melting temperature of the phase change material dispersed inside an emulsion.

References

1. Clause D, Pezron I, Gauthier A. Water transfer in mixed water-in-oil emulsions studied by differential scanning calorimetry. *Fluid Phase Equilib.* 1995;110(1-2):137-50.

2. Clause D, Gomez F, Pezron I, Komunjer L, Dalmazzone C. Morphology characterization of emulsions by differential scanning calorimetry. *Adv Colloid Interface Sci.* 2005;117(1-3):59-74.
3. Clause D, Gomez F, Dalmazzone C, Noik C. A method for the characterization of emulsions: Thermogravimetry - Application to water-in-crude oil emulsion. *J Colloid Interface Sci.* 2005;287:694-703.
4. Zhao ZN, Shi YQ. *J Eng Thermophys.* 2001;22:589-92.
5. Yang R, Xu H, Zhang Y. Preparation, physical property and thermal physical property of phase change microcapsule slurry and phase change emulsion. *Solar Energy Mater Solar Cells.* 2003;80(4):405-16.
6. Dalmazzone C, Noik C, Clause D. *Oil Gas Sci Technol - Rev. IFP,* 2008.
7. Zeraoui Y, Ehmimed J, Dumas JP. Modèles de transferts thermiques lors de la fusion d'une solution binaire dispersée. *Int J Therm Sci.* 2000;39(8):780-96.
8. Gibout S, Strub M, Dumas JP. Estimation of the nucleation probability in emulsions. *Int J Heat Mass Transf.* 2004;47(1):63-74.
9. Gibout S, Jamil A, Kousksou T, Zeraoui Y, Castaing-Lasvignottes J. Simulation of the thermal transfer during an eutectic melting of a binary solution. *Thermochim Acta.* 2006;441(1):30-4.

10. Kouksou T, Jamil A, Zeraouli Y, Dumas JP, Schall E. Isothermal and nonisothermal melting of the binary solution inside an emulsion. *Thermochim Acta*. 2007;460(1–2):22–7.
11. Jamil A, Kouksou T, Gibout S, Zeraouli Y, Dumas JP. DSC study and computer modelling of the melting process in ice slurry. *Thermochim Acta*. 2006;448(2):123–9.
12. Kouksou T, Jamil A, Zeraouli Y, Dumas JP. Experimental and modeling study of ice melting. *J Therm Anal Calorim*. 2007;89(1):31–6.
13. Timmermans J. *The physico-chemical constants of binary systems in concentrated solutions*, New York: Interscience Publishers; 1959–1960.